Bulgarian Chemical Communications, Volume 50 Special Issue D (pp. 55 – 61) 2018

Ionic Conductivity of Na-doped $SrSiO_3$

M. Viviani[1*], A. Barbucci[1,2], M. P. Carpanese[1,2], R. Botter[2], D. Clematis[2], S. Presto[1]

[1] *Institute of Condensed Matter Chemistry and Energy Technologies (ICMATE), National Council of Research (CNR), c/o DICCA-UNIGE, Via all'Opera Pia 15, 16145 Genova, Italy*

[2] *Department of Civil, Chemical and Environmental Engineering (DICCA), University of Genova, Via all'Opera Pia 15, 16145 Genova, Italy*

Received June 22, 2018 Revised September 1, 2018

The conductivity of a newly proposed ionic conductor Na-doped $SrSiO_3$ was studied. Powders were prepared by mixing of $SrCO_3$, Na_2CO_3 and SiO_2 in water or ethanol in order to explore the effect of solvents on the formation of secondary phases. X-ray diffraction was employed to study the phase composition of mixtures treated in air at different temperatures in the range 950-1050 C for 20 hours. Various heating schemes were applied to help the incorporation of Na in the monoclinic $SrSiO_3$ structure. Pressed pellets were sintered at 1000 °C for 20 hours and electroded with Ag paste for electrochemical characterization by impedance spectroscopy. For most compositions and thermal treatments, the formation of the insulating $Na_2Si_2O_5$ phase was observed as a matrix around grains of the monoclinic $SrSiO_3$ phase. Double calcination limited conductivity but increased its thermal stability. When ethanol was used for powder mixing, the material exhibited higher conductivity after long term ageing at 650 °C, also thanks to its low activation energy, without appreciable crystallization of other silicates

Key words: Ionic conductors, silicates, conductivity

INTRODUCTION

During last decades a lot of efforts have been spent to improve performances of Solid Oxide Fuel Cells (SOFC), and particularly to lower the operative temperature down to the 600 °C range. Some of them aimed to new designs [1-7]; other regarded the development of new materials [8, 8-11].

Recently, there has been some interest about alkali–doped $SrSiO_3$ and $SrGeO_3$ as oxide ion conductors with possible application as electrolyte materials in SOFC. In a series of papers [12,13] the formation of solid solutions, without any secondary phases, and with conductivity exceeding 0.05 S cm at 600 °C in air was reported.

Conductivity was ascribed to migration of oxygen vacancies, formed as an effect of replacement of Sr^{2+} with Na^+ ions [14].

Those findings were objected by several reports that pointed out the crucial role of glassy phases from the Na_2O–SiO_2 system [15- 17].

In particular, solid-state NMR spectroscopy studies allowed to associate conduction of SNS to migration of Na^+ ions in the amorphous phase [19, 20] and XRD analyses evidenced the very limited incorporation of Na into $SrSiO_3$ [21,22]. Conductivity also appeared to be strongly dependent on the crystallization of $Na_2Si_2O_5$ after some treatment at temperatures around 650 °C [21,23].

Some authors have reported the effect of synthesis method and processing conditions on the structure and conducting properties of alkali–doped $SrSiO_3$ and $SrGeO_3$. Alternatively to the conventional solid–state route, freeze drying of homogenous solutions of all cations was reported, resulting in more crystalline powders and in ceramics with lower conductivity [23].

Powders prepared by solid–state route were also sintered by spark plasma (SPS), which allowed obtaining single phase materials, with fine grains and with relatively high ionic conductivity [25].

From this brief summary, it appears that phase composition and consequently electrical properties must be highly sensitive to processing, particularly to reaction conditions of precursors and to the thermal history. In order to get insight on such aspects, the effects of some processing parameters, like the mixing medium and thermal treatments, have been studied for Na doped $SrSiO_3$ and results are reported in this paper.

EXPERIMENTAL

Powders with nominal composition $Sr_{1-x}Na_xSiO_3$ ($0.1 \leq x \leq 0.45$), denoted as SNSX, were prepared by the solid–state route, starting from $SrCO_3$, Na_2CO_3

To whom all correspondence should be sent:
E-mail: massimo.viviani@cnr.it

and SiO_2. Three dispersing liquids with different polarity (acetone, ethanol and distilled water) were employed in order to explore the effect of solvent on Na incorporation and glassy phase formation. After milling and freeze–drying calcination was carried out in air in order to get the final product following the reaction:

$$(1\text{-}x)SrCO_3+\frac{x}{2}Na_2CO_3+SiO_2 \rightarrow Sr_{(1-x)}Na_xSiO_{3-\frac{x}{2}}+\left(1-\frac{x}{2}\right)CO_2 \quad (1)$$

In case of acetone, four compositions with x = 0.1, 0.2, 0.3 and 0.4 were prepared, while in case of ethanol and water the composition reported with highest conductivity (x = 0.45) [0] was prepared only.

Powders were treated one or two times at temperatures ranging between 850 and 1050 °C and manually grinded after each thermal treatment. The details of all treatments are reported in Table 1.

Table 1. Thermal treatments applied to different compositions. Note that X = 100 x

SNSXa X = 10–40 acetone	SNS45e / SNS45w ethanol / water
A = 850 °C / 12 h	C = 1050 °C /20 h
B = A + 1000 °C /12 h	D = C + 950 °C /20 h
	E = C + D + 1000 °C /20 h

All compositions were also "aged" in air for 150 h at 650 °C in order to check their stability, and particularly to allow for crystallization or devitrification of any glassy phase.

Phase composition of powders was investigated by XRD (CubiX − Panalytical, Cu-K_α radiation, $\Delta 2\theta$ = 0.02 deg, integration = 7 sec/point) and morphology was observed by SEM (1450VP − LEO).

Ceramics were obtained by sintering at 1000 °C (see Table 1, treatments B and E) disk-shaped pellets which were prepared by uniaxial pressing. Microstructure was investigated by SEM (Phenom XL, Phenom World) on polished cross sections. Electrodes for electrical characterization were realized by brushing Ag paste (Euroinks) on both sides, followed by curing at 700°C for 30 min.

Electrochemical Impedance Spectroscopy (EIS) was carried out in laboratory air at different temperatures within a custom test rig and employing an automatic Frequency Response Analyzer (Iviumstat H, IVIUM). Spectra were collected each 25 °C during heating and cooling between room temperature and 650 °C. A 150h–long ageing at 650 °C enabled studying the dependence of conductivity on time for samples SNS40a and SNS45e.

RESULTS AND DISCUSSION

Na_2CO_3 is known to be highly soluble in water, weakly soluble in ethanol and insoluble in acetone. Therefore, the use of different dispersing media is expected to result in a different spatial distribution of Na within unreacted mixtures before calcination. In addition, some dissolution of Si into alkaline Na_2CO_3 solution at room temperature has to be taken into account [25], as well as the presence of strongly bonded hydroxyls due to the interaction between water, silica and Na_2CO_3.

XRD profiles of all SNSX powders are presented in Fig. 1 and observed phases are summarized in Table 2.

After the first treatment (calcination, A or C) all samples, reported in Fig. 1(i), contained only one crystalline phase, corresponding to the structure of $SrSiO_3$, with monoclinic symmetry (S.G. C2/c, JCPDS card 01-077-0233). Some flat−top parts can be detected in the diffraction profile of samples with lower Na amount (< 30 at. %) and of the powder prepared in ethanol (SNS45e). These features (marked with an asterisk) suggest the presence of amorphous or nanocrystalline regions. It is worth noting that for other samples minor peaks of the $SrSiO_3$ phase appear in the same parts of the profile.

Additional thermal treatments, as reported in Table 2, allowed for either the formation of new phases or crystallization of amorphous regions. In particular, for powders prepared in acetone the phase $Na_2Si_2O_5$ (JCPDS card 29-1261 and/or JCPDS card 22-1397) was found in compositions with higher Na content (≥30 at. %). In case of further aging at 650 °C, Na_2SiO_3 (JCPDS card 16-0818) was also detected in addition to two different forms of $Na_2Si_2O_5$, as can be seen in Fig.1(ii) for SNS40a. This is in agreement with several papers about SNS prepared with the same procedure, reporting the presence of glassy $Na_2Si_2O_5$, which could be devitrified after heating at T > 600 °C [20, 22]. For water- and ethanol-based preparations, aging of as-calcined powders resulted in crystallization of sodium silicate phase (JCPDS card 23-0529) as in case of acetone. On the contrary, a second thermal treatment at 950 °C deeply affected the resulting phase composition.

As can be seen in Figs. 1(iii-iv), aging at 650 °C caused the formation of $Na_2SrSi_2O_6$ (JCPDS card 32-1159) in both samples, showing that Na was partially incorporated in ternary oxide instead of the glassy $Na_2Si_2O_5$. Ageing of ceramics, i.e. after

sintering stage, introduced a difference between SNS45w and SN45e, and with the former being decomposed in several sodium silicates (see Fig. 1(iii) and the latter showing no evidence of any secondary phase (see Fig. 1(iv)

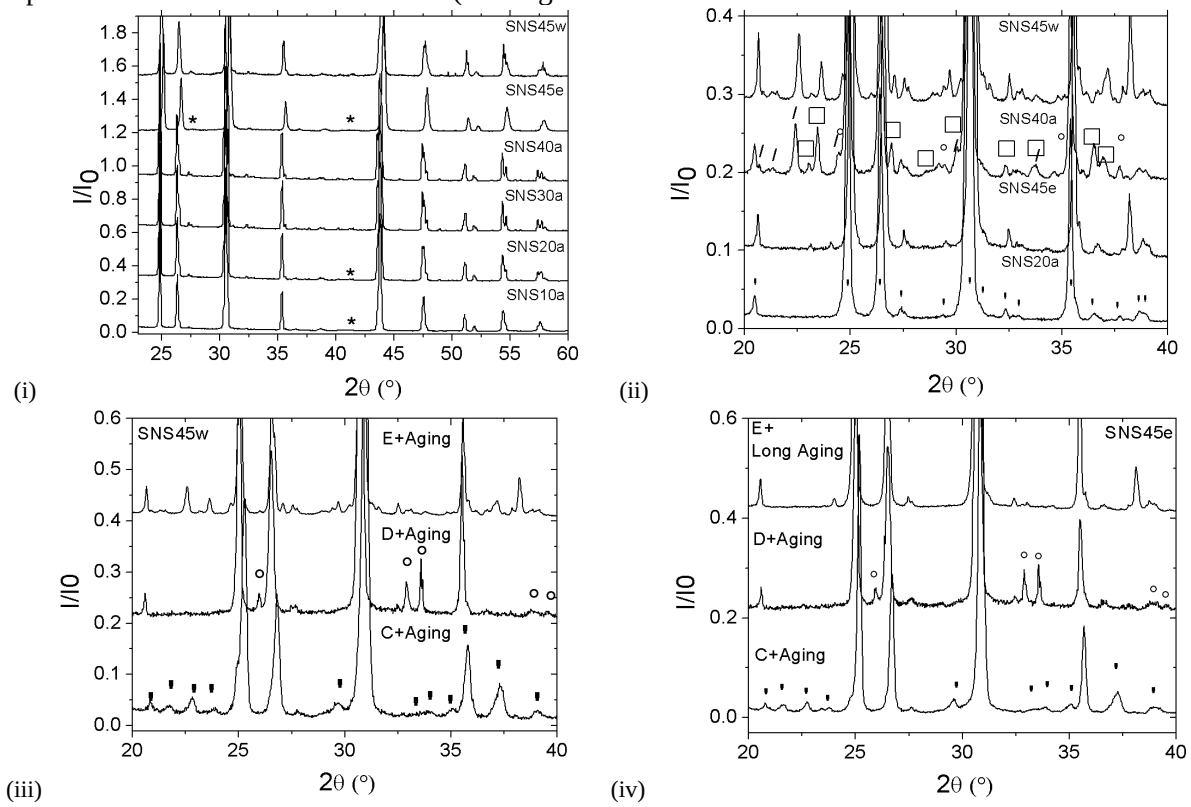

Fig. 1. XRD of SNSX. All compositions after thermal treatment at 850 °C or 1050 °C, * = amorphous or nanocrystalline regions (i); compositions as reported in label after EIS measurement, ' = $SrSiO_3$, ° = Na_2SiO_3, □ = α–$Na_2Si_2O_5$ (ii), SNS45w (iii) and SNS45e (iv), after ageing at 650 °C (°)=$Na_2SrSi_2O_6$, (')= $Na_2Si_2O_5$

Table 2. Activation Energy (E_a), conductivity value calculated @ 600°C and phase composition (JCPDS card numbers in brackets) of SNSX after different thermal treatments.

Sample	E_a **(eV)**	**Treatment**	**Phases**	**σ(S cm^{-1}) @600°C**
SNS10a		A	$SrSiO_3$ (01-077-0233)	
	1.89	B	$SrSiO_3$ (01-077-0233)	$2.6\ 10^{-5}$
SNS20a		A	$SrSiO_3$ (01-077-0233)	
	1.37	B	$SrSiO_3$ (01-077-0233)	$2.2\ 10^{-4}$
SNS30a		A	$SrSiO_3$ (01-077-0233)	
	1.33	B	$SrSiO_3$ (01-077-0233), $Na_2Si_2O_5$ (29-1261)	$9.5\ 10^{-4}$
SNS40a		A	$SrSiO_3$ (01-077-0233)	
	1.30	B		$2.9\ 10^{-3}$
		B+650 °C/150 h	$SrSiO_3$ (01-077-0233), $Na_2Si_2O_5$ (22-1397), $Na_2Si_2O_5$ (29-1261), Na_2SiO_3 (16-0818)	
SNS45w		C	$SrSiO_3$ (01-077-0233)	
		C+650 °C/150 h	$SrSiO_3$ (01-077-0233), $Na_2Si_2O_5$ (23-0529)	
		D+650 °C/150 h	$SrSiO_3$ (01-077-0233), $Na_2SrSi_2O_6$ (32-1159)	
	0.62	E		$7.6\ 10^{-6}$
		E+650 °C/150 h	$SrSiO_3$ (01-077-0233), $Na_2Si_2O_5$ (22-1397), $Na_2Si_2O_5$ (23-0529), Na_2SiO_3 (16-0818)	
SNS45e		C	$SrSiO_3$ (01-077-0233)	
		C+650 °C/150 h	$SrSiO_3$ (01-077-0233), $Na_2Si_2O_5$ (23-0529)	
		D+650 °C/150 h	$SrSiO_3$, $Na_2SrSi_2O_6$ (32-1159)	
	0.52	E		$1.7\ 10^{-4}$
		E+650 °C/150 h	$SrSiO_3$ (01-077-0233)	
		E+650 °C/300 h	$SrSiO_3$ (01-077-0233)	

SEM observation (backscatter mode) of cross sections of ceramics aged during electrical testing are reported in Fig. 2. Both SNS40a (i) and SNS45w (ii) show light grains with rounded shape immersed into a matrix with darker shades. EDAX analyses indicate that grains correspond to $SrSiO_3$ containing less than 5 at. % of Na, while matrix region composition is close to $Na_2Si_2O_5$ (light grey areas) and Na_2SiO_3 (dark grey areas).

The microstructure of SNS45e also is characterized by coexistence of light rounded grains, that were identified as corresponding to $SrSiO_3$ by EDAX analyses, and dark matrix. Differently from previous samples, in this case the matrix appears homogenous (white spots are Ag particles from electrodes) and therefore with one single composition (Fig. 2iv). Because XRD did not revealed other phases beyond $SrSiO_3$, this dark matrix is a glassy phase, still not crystallized after 300h (see fig. 2iv).

The electrical characterization was carried out in air by impedance spectroscopy, that is a very powerful technique when the appropriate corrections are applied [25].

An example of the results is presented in Fig. 3, where data collected at 500 °C for the SNS45e sample are represented as Nyquist plot.

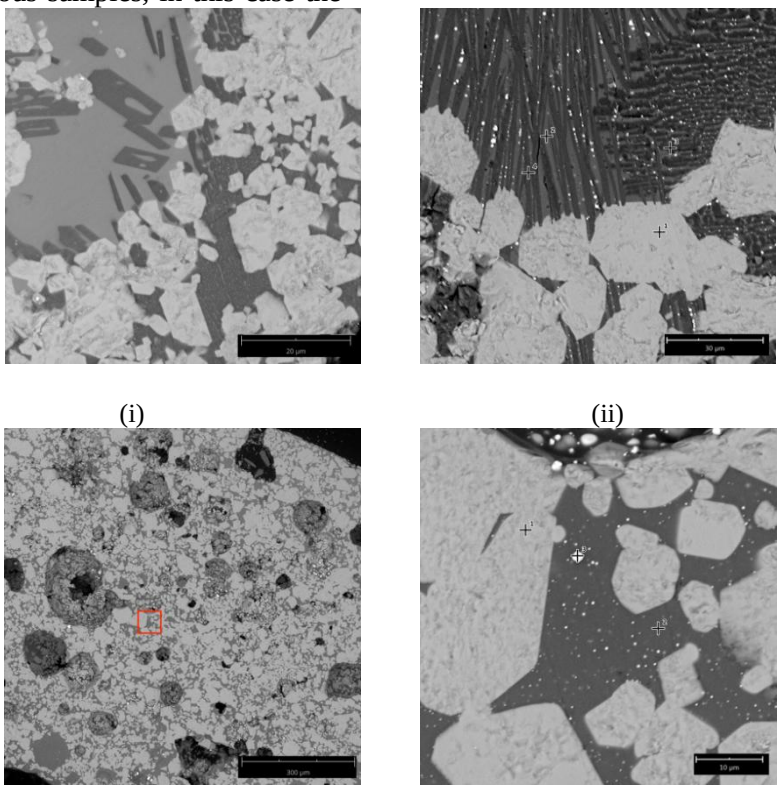

(i) (ii)

(iii) (iv)

Fig. 2. SEM backscatter on cross section of ceramics aged along electrical testing. SNS40a (i), SNS45w (ii), SNS45e (iii, iv). Red square in (iii) locates the area shown in (iv) at higher magnification.

The spectrum shows one semicircle, which is assigned to the electrolyte, and one feature at low frequency which can be considered contribution from electrodes. For the purpose of this work, low frequency intercept of the spectrum with real axis was considered as total resistance of samples. Those values were used to calculate the conductivity by using the Ohm's law.

From data reported in Table 2, it can be noted that for samples prepared in acetone, increasing the amount of Na leads to materials with increased conductivity and decreased E_a. On the contrary, materials prepared in ethanol or water shows much lower conductivity and lower E_a.

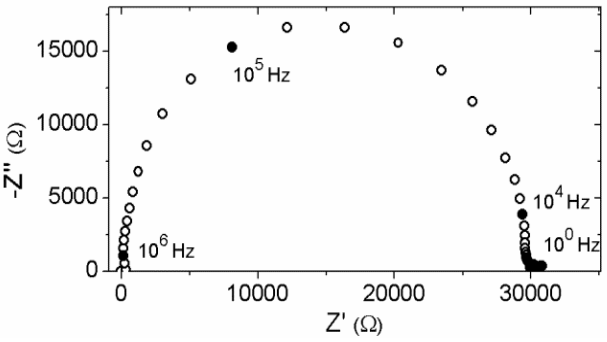

Fig. 3. Nyquist plot of SNS45e at 500 °C. Frequency decades are marked on the plot.

The activation energy of SNS is reported to be between 0.3 and 0.5 eV [0,12], while for both glassy and crystalline $Na_2Si_2O_5$ much larger values were measured (≥ 1.1 eV) [20,20].

By comparing literature data with present results, it is therefore possible to assimilate SNSXa to $Na_2Si_2O_5$. On the contrary, activation energy for conduction in SNS45e and SNS45w is closer to that of Na-doped $SrSiO_3$, although the conductivity is limited by considerable amount of glassy regions.

This is further confirmed by ageing behaviour of conductivity, presented in Fig. 4. The conductivity of SNS40a is strongly lowered by dwelling, which can be ascribed to the crystallization of $Na_2Si_2O_5$.

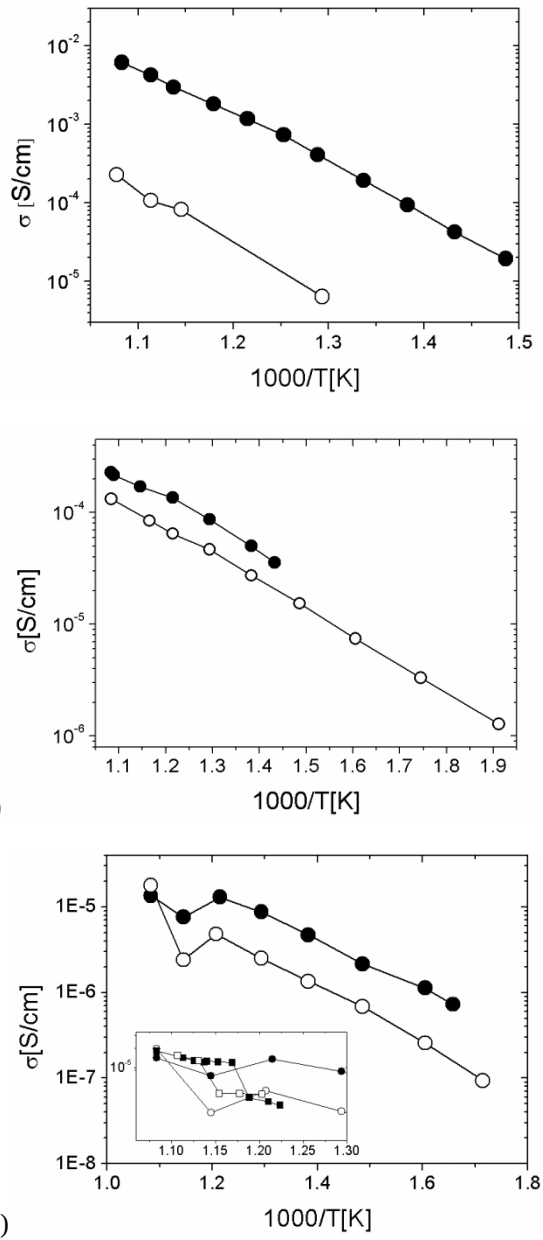

Fig. 4. Arrhenius plots of total conductivity during heating (red) and cooling after ageing (650 °C / 150 h) (blue) for SNS40a (i) SNS45e (ii) and SNS45w (iii).

This is not the case of SNS45e, were only a slight reduction of conductivity is observed after 150 h ageing. Accordingly, the crystallization of new phases was not observed for this sample. The conductivity of sample SNS45w shows some anomalies at temperatures between 550 and 650 °C, which are shown in Fig. 4iii. Inset also shows a second thermal cycle, which suggests the presence of a transition in that temperature range. The transition might be associated to glass crystallization, which is also supported by the acicular shape of Na-rich phases in this sample (Fig. 2ii).

From results reported above, it appears that processing can significantly modify the phase composition and the electrical properties of Na-doped $SrSiO_3$. XRD and SEM showed that Na incorporation in the monoclinic $SrSiO_3$ structure by the mechanism of eq. 1 is unfavourable, at least under the conditions explored in this work. Secondary phases from the Na_2O-SiO_2 system were detected in all materials with Na content higher than 20 at. %, and always present as amorphous regions. Ageing at 650 °C was effective in promoting crystallization of glassy phase in near all samples. An exception is represented by the samples processed with double calcination before sintering. Ageing at 650 °C for 150 h carried out after the second calcination revealed the formation of the 1:1 phase from the $SrSiO_3$–Na_2SiO_3 system ($Na_2SrSi_2O_6$), suggesting a beneficial effect from the double thermal treatment towards simultaneous incorporation of Na and Sr. In case of ethanol processing (SNS45e), further heat treatment at high temperature (sintering) was effective in stabilizing the amorphous regions which did not crystallize even after prolonged ageing (300 h) at 650 °C. This might be due to the composition of the glass as it is known that crystallization of alkali-silicates with high Si concentration is kinetically limited due to the high viscosity around the melting point [27]. Further investigation would be needed to clarify this aspect.

For the SNS45e sample, it is not possible to conclude whether the SNS or the glass are contributing to conduction. Given that only one semicircle is present in impedance diagrams, separation of two contributions is not possible. The very low total conductivity associated to low activation energy make this composite quite different from all previously reported about SNS.

For water processing (SNS45w), much lower conductivity was obtained and stabilization could not be achieved (see Table 2). Therefore, in this case a lower Si/Na molar ratio is expected in the

matrix or, in other terms, a lower incorporation of Na in the $SrSiO_3$ phase.

CONCLUSIONS

The effects of preparation and thermal treatment conditions on properties of $Sr_{1-x}Na_xSiO_3$, with $0.1 \leq x \leq 0.45$, were studied. The preparation was carried out by solid−state route with three different mixing media. Acetone, ethanol and water were selected for their large difference in polarity and therefore for the different solubility of Na_2CO_3. Calcination was carried out under different conditions, by changing temperature and number of treatments. Results from X-ray diffraction, SEM-EDAX and impedance spectroscopy confirmed that the Na-$SrSiO_3$ system is always a multi-phase structure, with some amount of sodium silicates (amorphous or crystalline) increasing with Na concentration. Quantity and crystallinity of sodium silicates determines both the level of conductivity and its thermal stability. Highest conductivity and degradation rate was obtained when synthesis was carried out in acetone with single calcination step at 850 °C. Double calcination limited conductivity but increased its thermal stability. When ethanol was used for powder mixing and double calcination was applied, the material exhibited higher conductivity after long term ageing at 650 °C also thanks to its low activation energy, without appreciable crystallization of other silicates. Such results make the ethanol-based preparation promising for the realization of a stable material suitable as electrolyte material in SOFC.

REFERENCES

1. Su, S.; Gao, X.; Zhang, Q.; Kong, W.; Chen, D., Anode- Versus Cathode-Supported Solid Oxide Fuel Cell: Effect of Cell Design on the Stack Performance. *Int. J. Electrochem. Sci*., **10**, 2487 (2015).
2. Thorel, A. S.; Abreu, J.; Ansar, S.-A.; Barbucci, A.; Brylewski, T.; Chesnaud, A.; Ilhan, Z.; Piccardo, P.; Prazuch, J.; Presto, S.; Przybylski, K.; Soysal, D.; Stoynov, Z.; Viviani, M.; Vladikova D. Proof of concept for the dual membrane cell I. Fabrication and electrochemical testing of first prototypes. Journal of *The Electrochemical Society*, **160(4)**, F360 (2013).
3. Presto, S.; Barbucci, A.; Viviani, M.; Ilhan, Z.; Ansar, S.-A.; Soysal, D.; Thorel, A. S.; Abreu, J.; Chesnaud, A.; Politova, T.; Przybylski, K.; Prazuch, J.; Brylewski, T.; Zhao, Z.; Vladikova, D.; Stoynov Z. IDEAL-Cell, innovative dual membrane fuel-cell: fabrication and electrochemical testing of first prototypes. *ECS Transactions*, , **25(2)**, 773 (2009).
4. Xu, J. ; Zhou, X.; Cheng, J.; Pan, L.; Wu; M.; Dong, X.; Sun, K. Electrochemical performance of highly active ceramic symmetrical electrode La0.3Sr0.7Ti0.3Fe0.7O3-δ-CeO2 for reversible solid oxide cells. *Electrochimica Acta*, **257**, 64 (2017).
5. Krishnan, V. V. Recent developments in metal-supported solid oxide fuel cells. *WIREs Energy Environ*, **6**:e246, 1 (2017).
6. Viviani, M., Canu, G., Carpanese, M.P., Barbucci, A., Sanson, A., Mercadelli, E., Nicolella, C., Vladikova, D., Stoynov, Z., Chesnaud, A., Thorel, A., Ilhan, Z., Ansar, S.-A., *Energy Procedia*, **28**, 182 (2012).
7. Vladikova, D., Stoynov, Z., Chesnaud, A., Thorel, A., Viviani, M., Barbucci, A., Raikova, G., Carpanese, P., Krapchanska, M., Mladenova, E., *International Journal of Hydrogen Energy*, **39(36)**, 21561 (2014).
8. N. Mahato, A. Banerjee, A. Gupta, S. Omar, K. Balani, Progress in Materials Science Progress in material selection for solid oxide fuel cell technology : A review, *Prog. Mater. Sci*. **72**, 141 (2015).
9. Carpanese, M.P., Barbucci, A., Canu, G., Viviani, M., *Solid State Ionics*, **269**, 80 (2015).
10. Giuliano, A., Carpanese, M.P., Panizza, M., Cerisola, G., Clematis, D., Barbucci, A., *Electrochimica Acta*, **240**, 258 (2017).
11. S. Presto, A. Barbucci, M. P. Carpanese, M. Viviani, R. Marazza, *J. Appl. Electrochem.*, **39**, 2257 (2009).
    P. Singh, J.B. Goodenough, $Sr_{1-x}K_xSi_{1-y}Ge_yO_{3-0.5x}$: a new family of superior oxide-ion conductors, *Energy Environ. Sci*. **5**, 9626 (2012).
12. P. Singh, J.B. Goodenough, Monoclinic Sr 1– x Na x SiO 3–0.5 x : New Superior Oxide Ion Electrolytes, *J. Am. Chem. Soc.* **135,** 10149 (2013).
13. T. Wei, P. Singh, Y. Gong, J.B. Goodenough, Y. Huang, K. Huang, $Sr_{3-3x}Na_{3x}Si_3O_{9-1.5x}$ (x = 0.45) as a superior solid oxide-ion electrolyte for intermediate temperature-solid oxide fuel cells, *Energy Environ. Sci.* **7,** 1680 (2014).
14. R. Martinez-Coronado, P. Singh, J. Alonso-Alonso, J.B. Goodenough, R. Martinez, J.A. Alonso, Structural investigation of the oxide-ion electrolyte with SrMO3 (M = Si/Ge) structure, *J. Mater. Chem.* A. **2,** 4355 (2014).
15. R.D. Bayliss, S.N. Cook, S. Fearn, J.A. Kilner, C. Greaves, S.J. Skinner, On the oxide ion conductivity of potassium doped strontium silicates, *Energy Environ. Sci*. **7**, 2999 (2014).
16. K. Sood, S. Basu, Co-existence of amorphous and crystalline phases in Na-doped SrSiO 3 system, *RSC Adv*. **6,** 20211 (2016).
17. I.R. Evans, J.S.O. Evans, H.G. Davies, A.R. Haworth, M.L. Tate, On Sr1–x Na x SiO3–0.5 x New Superior Fast Ion Conductors, *Chem. Mater.* **26**, 5187 (2014).
18. K.K. Inglis, J.P. Corley, P. Florian, J. Cabana, R.D. Bayliss, F. Blanc, Structure and Sodium Ion Dynamics in Sodium Strontium Silicate Investigated by Multinuclear Solid-State NMR, *Chem. Mater.* **28**, 3850 (2016)
19. P.-H. Chien, Y. Jee, C. Huang, R. Dervişoğlu, I. Hung, Z. Gan, K. Huang, Y.-Y. Hu, On the origin of high ionic conductivity in Na-doped SrSiO 3, *Chem. Sci*. **7**, 3667 (2016).

20. C. Tealdi, L. Malavasi, I. Uda, C. Ferrara, V. Berbenni, P. Mustarelli, Nature of conductivity in SrSiO3-based fast ion conductors., *Chem. Commun.* **50**, 14732 (2014).
21. Y. Jee, X. Zhao, K. Huang, On the cause of conductivity degradation in sodium strontium silicate ionic conductor., *Chem. Commun.* **51**, 9640 (2015).
22. Y. Jee, X. Zhao, X. Lei, K. Huang, Phase Relationship and Ionic Conductivity in Na-SrSiO 3 Ionic Conductor, *J. Am. Ceram. Soc*. **99**, 324 (2016).
23. S. Fernández-Palacios, L. do. Santos-Gómez, J.M. Compana, J.M. Porras-Vázquez, A. Cabeza, D. Marrero-López, E.R. Losilla, Influence of the synthesis method on the structure and electrical properties of Sr1−xKxGeO3−x/2, *Ceram. Int.* **41**, 6542 (2015).
24. F. Yang, Z. Yu, B. Meng, Y.J. Zhu, Q.Q. Yang, Z.L. Lin, H.M. Zhou, X.L. Liang, Microstructure and electrical properties of $Sr_{1-x}Na_xSiO_{3-x/2}$ ceramics prepared by SPS process, *Ionics (Kiel)*. **22**, 2087 (2016).
25. S.S. Jørgensen, The application of alkali dissolution techniques in the study of cretaceous flints, *Chem. Geol.* **6**, 153 (1970).
26. G. Raikova, M. P. Carpanese, Z. Stoynov, D. Vladikova, M. Viviani, A. Barbucci, *Bulg. Chem. Commun*., **41**, 199 (2009).
27. M.W. Barsoum, Fundamentals of ceramics, second, IOP Publishing Ltd, 2003, pp. 280-281.

Йонна проводимост на $SrSiO_3$ дотиран с натрий

М. Вивиани[1 *], А. Барбучи[1,2], М.П. Карпанезе[1,2], Р. Ботер[2], Д. Клематис[2], С. Престо[1]

[1] Институт по химия на кондензираната материя и енергийни технологии, Национален съвет по научни изследвания, Виа але Опера Пиа 15, 16145 Генуа, Италия
[2] Катедра по гражданско, химическо и екологично инженерство, Университет на Генуа, Виа але Опера Пиа 15, 16145 Генуа, Италия

Постъпила на.22 юни 2018г.; приета на 1 септгември 2018г.

(Резюме)

Изследвана е проводимостта на ново-открития йонен проводник $SrSiO_3$ дотиран с натрий. Чрез смесване на $SrCO_3$, Na_2CO_3 и SiO_2 бяха приготвени прахове във водна или етанолна среда, за да се проучи ефекта на разтворителите върху образуването на вторични фази. Използвана беше рентгенова дифракция за да се установи фазовия състав на смесите, третирани на въздух при различни температури в диапазона 950-1050 °C в продължение на 20 часа. Различни схеми на нагряване бяха приложени с цел да се подпомогне вграждането на Na в моноклинната $SrSiO_3$ структура. Пресованите таблетки се синтероват при 1000 °C в продължение на 20 часа и се покриват със сребърна паста за електрохимично характеризиране чрез импедансна спектроскопия. При повечето състави и термични обработки, образуването на изолираща фаза от $Na_2Si_2O_5$ се наблюдава като матрица от $SrSiO_3$ зърна в моноклинна фаза. Проводимостта е ограничена от двойно калциране, но се увеличава термичната стабилност. Когато се използва етанол за смесване на праховете, след дългосрочно стареене при 650 °C материалът има по-висока проводимост, също и по-ниска активационна енергия, без забележима кристализация на други силикати.